

HENRY

Hydraulic Engineering Repository

Ein Service der Bundesanstalt für Wasserbau

Conference Paper, Published Version

Shinohara, Kazunori; Okuda, Hiroshi

Shape Optimization Using Adjoint Variable Method in Incompressible Viscous Flow

Zur Verfügung gestellt in Kooperation mit/Provided in Cooperation with:
Kuratorium für Forschung im Küsteningenieurwesen (KFKI)

Verfügbar unter/Available at: <https://hdl.handle.net/20.500.11970/110230>

Vorgeschlagene Zitierweise/Suggested citation:

Shinohara, Kazunori; Okuda, Hiroshi (2008): Shape Optimization Using Adjoint Variable Method in Incompressible Viscous Flow. In: Wang, Sam S. Y. (Hg.): ICHE 2008. Proceedings of the 8th International Conference on Hydro-Science and Engineering, September 9-12, 2008, Nagoya, Japan. Nagoya: Nagoya Hydraulic Research Institute for River Basin Management.

Standardnutzungsbedingungen/Terms of Use:

Die Dokumente in HENRY stehen unter der Creative Commons Lizenz CC BY 4.0, sofern keine abweichenden Nutzungsbedingungen getroffen wurden. Damit ist sowohl die kommerzielle Nutzung als auch das Teilen, die Weiterbearbeitung und Speicherung erlaubt. Das Verwenden und das Bearbeiten stehen unter der Bedingung der Namensnennung. Im Einzelfall kann eine restriktivere Lizenz gelten; dann gelten abweichend von den obigen Nutzungsbedingungen die in der dort genannten Lizenz gewährten Nutzungsrechte.

Documents in HENRY are made available under the Creative Commons License CC BY 4.0, if no other license is applicable. Under CC BY 4.0 commercial use and sharing, remixing, transforming, and building upon the material of the work is permitted. In some cases a different, more restrictive license may apply; if applicable the terms of the restrictive license will be binding.

SHAPE OPTIMIZATION USING ADJOINT VARIABLE METHOD IN INCOMPRESSIBLE VISCOUS FLOW

Kazunori Shinohara¹ and Hiroshi Okuda²

¹ Researcher, Intelligent Modelling Laboratory, The University of Tokyo
2-11-16, Yayoi, Bunkyo-ku, Tokyo, 113-8656, Japan, e-mail: sinohara@nihonbashi.race.u-tokyo.ac.jp

² Professor, Research into Artifacts, Center for Engineering, The University of Tokyo
5-1-5, Kashiwanoha, Kashiwa, Chiba, 277-8568, Japan, e-mail: okuda@race.u-tokyo.ac.jp

To maximize the lift and to reduce the drag of an object placed under Stokes flow, a 3D shape optimization system based on the adjoint variable method was developed by using HEC-MW. The adjoint variable method is based on the Lagrange multiplier method (a conditional variational principle), and consists of the state equation, the adjoint equation and the sensitivity equation. In this context, the equations for increasing the lift, under a constant volume condition, are formulated. By deforming from the initial shape to the optimal shape, the lift coefficient of the object has been increased and the drag coefficient has been decreased.

Keywords: Shape optimization, CFD, FEM, HEC-MW, Adjoint variable method, Navier-Stokes equation, Calculus of variations

1. INTRODUCTION

The literature has discussed the minimizing drag and the maximizing lift for the airplane wing since the 1970's (Hicks, 1974; Jameson, 1988). When a wing moves in the air, the lift of the wing increases in proportion to the square of the speed. However, as the speed for the wing increases, the drag on the wing increases as well. Therefore, if the wing is not properly designed, the airplane can't obtain enough lift to counteract the drag. The optimal wing shape should provide both maximum lift and minimum drag, and not only one of them. Also, in most practical engineering problems, a device has to be designed to satisfy not one but more goals. Therefore the issue of multipurpose optimization becomes important. In this study we propose a multipurpose optimization method based on the adjoint variable method, which is a type of sensitivity analysis, and is based on the calculus of variations (Gelfand, 1963; Robert, 1974). The constrained optimization problem of the cost functional is converted into an unconstrained optimization of the Lagrange function by introducing Lagrange multipliers called adjoint variables. As an application of the proposed multipurpose optimization system using the adjoint variable method, we present a method for simultaneously minimizing drag and maximum lift.

2. ADJOINT VARIABLE METHOD

To minimize the cost function under constraints, we formulated the Lagrange function by introducing the adjoint variables. The adjoint variable method is based on the variational method. By introducing Lagrange multipliers called adjoint variables, the constrained optimization of the cost function is transformed to the unconstrained optimization of the Lagrange function. A circular cylinder is placed in the computational domain Ω , as shown in Fig.1. Γ is the *N-S-E-W* boundary at north, south, east and west. γ represents the surface of the object under optimization. A fluid flows in on the boundary Γ_w and flows out on the boundary Γ_E . The origin of coordinates is at the centre of the cylinder. In this paper, as the cost function, the traction force on the surface γ is defined as:

$$\begin{aligned}
J &= -\int_{t_s}^{t_e} \int_{\gamma(\mathbf{x})} \left\{ -pn_1 + \frac{1}{\text{Re}} \left(\frac{\partial u_1}{\partial \chi_1} + \frac{\partial u_1}{\partial \chi_1} \right) n_1 + \frac{1}{\text{Re}} \left(\frac{\partial u_2}{\partial \chi_1} + \frac{\partial u_1}{\partial \chi_2} \right) n_2 + \frac{1}{\text{Re}} \left(\frac{\partial u_3}{\partial \chi_1} + \frac{\partial u_1}{\partial \chi_3} \right) n_3 \right\} d\gamma dt \\
&\quad - \int_{t_s}^{t_e} \int_{\gamma(\mathbf{x})} \left\{ -pn_2 + \frac{1}{\text{Re}} \left(\frac{\partial u_1}{\partial \chi_2} + \frac{\partial u_2}{\partial \chi_1} \right) n_1 + \frac{1}{\text{Re}} \left(\frac{\partial u_2}{\partial \chi_2} + \frac{\partial u_2}{\partial \chi_2} \right) n_2 + \frac{1}{\text{Re}} \left(\frac{\partial u_3}{\partial \chi_2} + \frac{\partial u_2}{\partial \chi_3} \right) n_3 \right\} d\gamma dt \\
&= -\int_{t_s}^{t_e} \int_{\gamma(\mathbf{x})} T_1 d\gamma dt - \int_{t_s}^{t_e} \int_{\gamma(\mathbf{x})} T_2 d\gamma dt \in \mathbf{R}^1
\end{aligned} \tag{1}$$

where t , \mathbf{x} , $\boldsymbol{\chi}$, \mathbf{n} , \mathbf{u} , \mathbf{T} and \mathbf{w} represents the time, the special coordinate, the coordinates in the integrand, the unit normal vector, the velocity vector, the traction vector and the state variable vector, respectively. The domain $\gamma(\mathbf{x})$ depends on \mathbf{x} . The constant t_s and t_e show the start of the test time and the end of the test time in the optimization. The constant Re represents the Reynolds number as follows:

$$\text{Re} = \frac{\rho L U_l}{\mu} \tag{2}$$

The constant L , U_l , ρ and μ denote the representative length and the representative flow, the density and the viscosity coefficient, respectively. In this paper, the equations are dimensionless. We formulated the Lagrange function by introducing the adjoint variable as follows:

$$L = J + B + V + F \in \mathbf{R}^1 \tag{3}$$

$$F = \int_{t_s}^{t_e} \int_{\Omega(\mathbf{x})} \lambda_1(t, \boldsymbol{\chi}) f_1(t, \boldsymbol{\chi}, \mathbf{W}(t, \boldsymbol{\chi})) d\Omega dt + \int_{t_s}^{t_e} \int_{\Omega(\mathbf{x})} \lambda_2(t, \boldsymbol{\chi}) f_2(t, \boldsymbol{\chi}, \mathbf{W}(t, \boldsymbol{\chi})) d\Omega dt \tag{4}$$

$$+ \int_{t_s}^{t_e} \int_{\Omega(\mathbf{x})} \lambda_3(t, \boldsymbol{\chi}) f_3(t, \boldsymbol{\chi}, \mathbf{W}(t, \boldsymbol{\chi})) d\Omega dt + \int_{t_s}^{t_e} \int_{\Omega(\mathbf{x})} \lambda_4(t, \boldsymbol{\chi}) f_4(t, \boldsymbol{\chi}, \mathbf{W}(t, \boldsymbol{\chi})) d\Omega dt \in \mathbf{R}^1$$

$$\begin{aligned}
B &= \int_{t_s}^{t_e} \int_{\Gamma_N(\mathbf{x}) + \Gamma_S(\mathbf{x})} \lambda_5(t, \boldsymbol{\chi}) T_1(t, \boldsymbol{\chi}, \mathbf{W}(t, \boldsymbol{\chi})) d\gamma dt + \int_{t_s}^{t_e} \int_{\Gamma_N(\mathbf{x}) + \Gamma_S(\mathbf{x})} \lambda_6(t, \boldsymbol{\chi}) u_2(t, \boldsymbol{\chi}) d\gamma dt \\
&+ \int_{t_s}^{t_e} \int_{\Gamma_N(\mathbf{x}) + \Gamma_S(\mathbf{x})} \lambda_7(t, \boldsymbol{\chi}) T_3(t, \boldsymbol{\chi}, \mathbf{W}(t, \boldsymbol{\chi})) d\gamma dt + \int_{t_s}^{t_e} \int_{\Gamma_U(\mathbf{x}) + \Gamma_L(\mathbf{x})} \lambda_8(t, \boldsymbol{\chi}) T_1(t, \boldsymbol{\chi}, \mathbf{W}(t, \boldsymbol{\chi})) d\gamma dt \\
&+ \int_{t_s}^{t_e} \int_{\Gamma_U(\mathbf{x}) + \Gamma_L(\mathbf{x})} \lambda_9(t, \boldsymbol{\chi}) T_2(t, \boldsymbol{\chi}, \mathbf{W}(t, \boldsymbol{\chi})) d\gamma dt + \int_{t_s}^{t_e} \int_{\Gamma_U(\mathbf{x}) + \Gamma_L(\mathbf{x})} \lambda_{10}(t, \boldsymbol{\chi}) u_3(t, \boldsymbol{\chi}) d\gamma dt
\end{aligned} \tag{5}$$

$$+ \int_{t_s}^{t_e} \int_{\Gamma_E(\mathbf{x})} \lambda_{11}(t, \boldsymbol{\chi}) T_1(t, \boldsymbol{\chi}, \mathbf{W}(t, \boldsymbol{\chi})) d\gamma dt + \int_{t_s}^{t_e} \int_{\Gamma_E(\mathbf{x})} \lambda_{12}(t, \boldsymbol{\chi}) T_2(t, \boldsymbol{\chi}, \mathbf{W}(t, \boldsymbol{\chi})) d\gamma dt$$

$$+ \int_{t_s}^{t_e} \int_{\Gamma_E(\mathbf{x})} \lambda_{13}(t, \boldsymbol{\chi}) T_3(t, \boldsymbol{\chi}, \mathbf{W}(t, \boldsymbol{\chi})) d\gamma dt$$

$$+ \int_{t_s}^{t_e} \int_{\Gamma_W(\mathbf{x})} \lambda_{14}(t, \boldsymbol{\chi}) \{u_1(t, \boldsymbol{\chi}) - 0.01\} d\gamma dt + \int_{t_s}^{t_e} \int_{\Gamma_W(\mathbf{x})} \lambda_{15}(t, \boldsymbol{\chi}) u_2(t, \boldsymbol{\chi}) d\gamma dt + \int_{t_s}^{t_e} \int_{\Gamma_W(\mathbf{x})} \lambda_{16}(t, \boldsymbol{\chi}) u_3(t, \boldsymbol{\chi}) d\gamma dt$$

$$+ \int_{t_s}^{t_e} \int_{\gamma(\mathbf{x})} \lambda_{17}(t, \boldsymbol{\chi}) u_1(t, \boldsymbol{\chi}) d\gamma dt + \int_{t_s}^{t_e} \int_{\gamma(\mathbf{x})} \lambda_{18}(t, \boldsymbol{\chi}) u_2(t, \boldsymbol{\chi}) d\gamma dt + \int_{t_s}^{t_e} \int_{\gamma(\mathbf{x})} \lambda_{19}(t, \boldsymbol{\chi}) u_3(t, \boldsymbol{\chi}) d\gamma dt \in \mathbf{R}^1$$

$$V = \kappa \int_{t_s}^{t_e} \int_{\Pi(\mathbf{x})} d\Omega dt \in \mathbf{R}^1 \tag{6}$$

where λ_1 shows the adjoint pressure corresponding to the pressure p and $(\lambda_2, \lambda_3, \lambda_4)$ show the adjoint velocity corresponding to the flow vector (u_1, u_2, u_3) . The control variables to deform the shape are the coordinates of the nodal points on the surface in the analytical model. The objective function consists of the cost function (J) and the function (V) representing the constant volume constraint imposed on the object. The shape is deformed to minimize this objective function. The variables λ_5 - λ_{19} represents the undetermined adjoint variables. The function $\mathbf{f}(t, \mathbf{x}, \mathbf{w}(t, \mathbf{x}))$ consists of the continuity equation $f_1(t, \mathbf{x}, \mathbf{w}(t, \mathbf{x}))$, the Stokes equation $f_2(t, \mathbf{x}, \mathbf{w}(t, \mathbf{x}))$, $f_3(t, \mathbf{x}, \mathbf{w}(t, \mathbf{x}))$, $f_4(t, \mathbf{x}, \mathbf{w}(t, \mathbf{x}))$. The Lagrange function is formulated

as follows:

$$\begin{aligned}
L = & J + B + V + \int_{t_s}^{t_e} \int_{\Omega(x)} \lambda_1 \left(\frac{\partial u_1}{\partial \chi_1} + \frac{\partial u_2}{\partial \chi_2} + \frac{\partial u_3}{\partial \chi_3} \right) d\Omega dt \\
& + \int_{t_s}^{t_e} \int_{\Omega(x)} \lambda_2 \left[-\frac{\partial u_1}{\partial t} - \frac{\partial p}{\partial \chi_1} + \frac{1}{\text{Re}} \left\{ 2 \frac{\partial}{\partial \chi_1} \frac{\partial u_1}{\partial \chi_1} + \frac{\partial}{\partial \chi_2} \left(\frac{\partial u_2}{\partial \chi_1} + \frac{\partial u_1}{\partial \chi_2} \right) + \frac{\partial}{\partial \chi_3} \left(\frac{\partial u_3}{\partial \chi_1} + \frac{\partial u_1}{\partial \chi_3} \right) \right\} \right] d\Omega dt \\
& + \int_{t_s}^{t_e} \int_{\Omega(x)} \lambda_3 \left[-\frac{\partial u_2}{\partial t} - \frac{\partial p}{\partial \chi_2} + \frac{1}{\text{Re}} \left\{ \frac{\partial}{\partial \chi_1} \left(\frac{\partial u_1}{\partial \chi_2} + \frac{\partial u_2}{\partial \chi_1} \right) + 2 \frac{\partial}{\partial \chi_2} \frac{\partial u_2}{\partial \chi_2} + \frac{\partial}{\partial \chi_3} \left(\frac{\partial u_3}{\partial \chi_2} + \frac{\partial u_2}{\partial \chi_3} \right) \right\} \right] d\Omega dt \\
& + \int_{t_s}^{t_e} \int_{\Omega(x)} \lambda_4 \left[-\frac{\partial w}{\partial t} - \frac{\partial p}{\partial \chi_3} + \frac{1}{\text{Re}} \left\{ \frac{\partial}{\partial \chi_1} \left(\frac{\partial u_1}{\partial \chi_3} + \frac{\partial u_3}{\partial \chi_1} \right) + \frac{\partial}{\partial \chi_2} \left(\frac{\partial u_2}{\partial \chi_3} + \frac{\partial u_3}{\partial \chi_2} \right) + 2 \frac{\partial}{\partial \chi_3} \frac{\partial u_3}{\partial \chi_3} \right\} \right] d\Omega dt \in \mathbf{R}^1
\end{aligned} \tag{7}$$

The integral domain depends on spatial coordinates. However, the domain $\gamma(x)$ etc. are often abbreviated to γ etc. The stationary conditions (the state equations, the adjoint equations and the sensitivity equations) are derived by using the first variation.

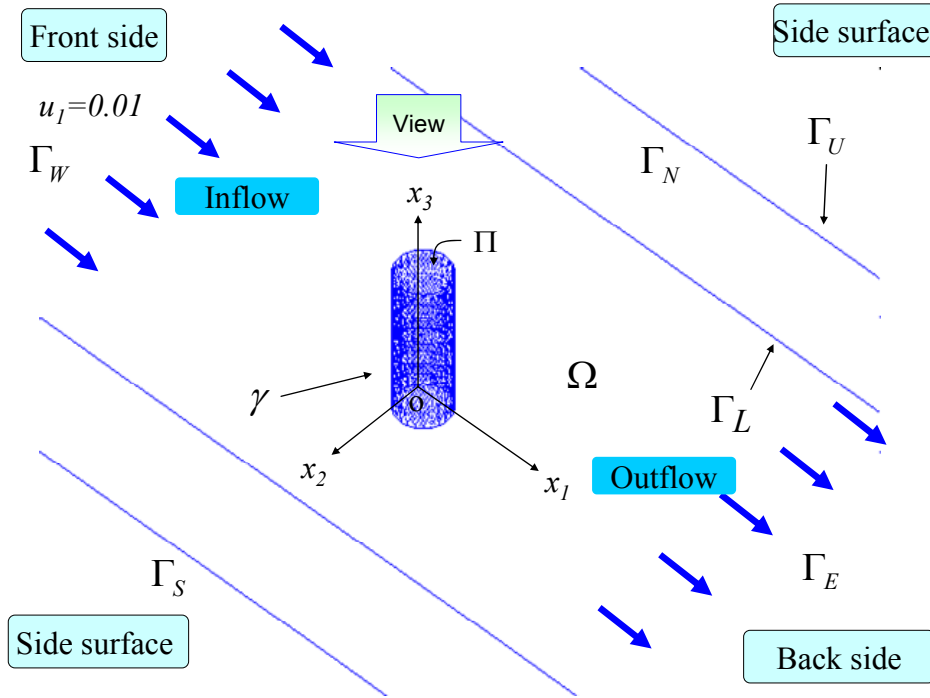


Fig.1 Computational domain.

3. ALGORITHM

In the first phase of the adjoint algorithm, the state equations are solved until the flow field reaches a steady state. The state variables are calculated by using the state equations, which are solved from the start-time to the end-time. All the nodal values of the state variables are stored at every time step. In the second phase, the adjoint variables are calculated by the adjoint equations from the end-time to the start-time. The adjoint equations are also advanced in time until the adjoint flow field reaches the steady state. All the nodal values of the adjoint variables are saved in files at every time step. In the third phase, the sensitivity at every time step is calculated by using the data saved in files containing the adjoint and state variables. This sensitivity represents the displacement of the nodes on the surface of the object. In the fourth phase, the shape is modified by using the sensitivity. The

optimization method used here is the gradient method. Afterwards, the nodes of the mesh are relocated according to the sensitivity. The node relocation is performed by using the biharmonic equation. In the fifth phase, the shape is modified such that the constraint of constant volume is satisfied

To overcome such difficulties as heavy computational burden and large memory requirements, the present system was implemented with the data compression technology supplied with the parallel software library HEC Middleware (Ito and Okuda, 2007). The HEC-MW is a hardware-independent platform, which includes patterns of calculation processes and common interfaces of unstructured grid simulations. By plugging-in HEC-MW, a program developed on a PC is automatically optimized for each high-end machine. Also, by utilizing HEC-MW, the program can be efficiently parallelized, and the number of program lines can be dramatically reduced. In connection to the shape optimization method, a mesh smoothing method, crucial to realizing the 3D shape optimization of the body surface, is developed. Based on the proposed method, a parallel 3D shape optimization algorithm is constructed and implemented using HEC-MW. For increased performance, a method that reduces the communication overhead is developed.

4. SHAPE OPTIMIZATION OF OBJECTS IN FLOW

The mesh is shown in Fig. 2. The mesh resolution is 15009 nodes and 67855 elements. The element type is 4-node tetrahedron element. The height of the cylinder is 0.3. In Fig.3 and Fig.4, the velocity vector and the pressure contour are shown. The flow speed (the state variable) decreases behind the downstream cylinder. The fluid flows from the inlet Γ_w to the outlet Γ_E . The adjoint velocity vector is shown in Fig.5. The boundary condition γ in the adjoint analysis is set to $(\lambda_2, \lambda_3, \lambda_4) = (1, 1, 0)$. This condition is naturally derived from the Lagrange function (Eq.(7)). In the artificial adjoint inflow on the cylinder, the adjoint flow vector has 45 degree with respect x_1 axis. The adjoint flow turns in the computational domain and finally reached the outlet where is the position in 225 degree with respect to x_1 axis.

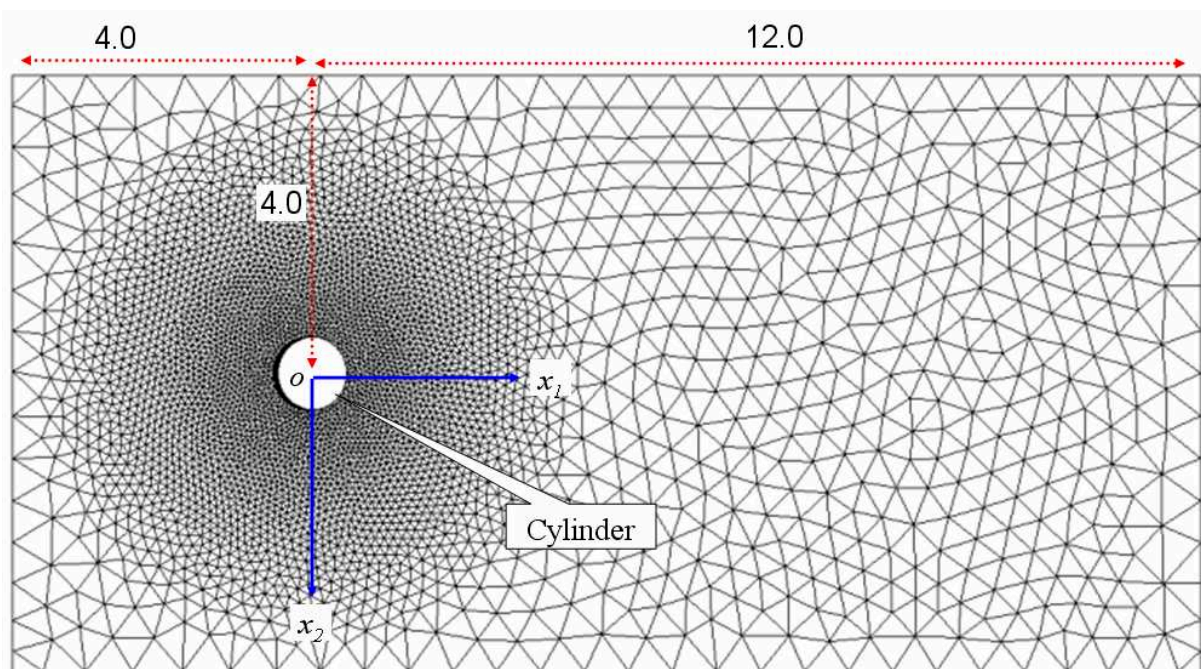


Fig.2 Mesh

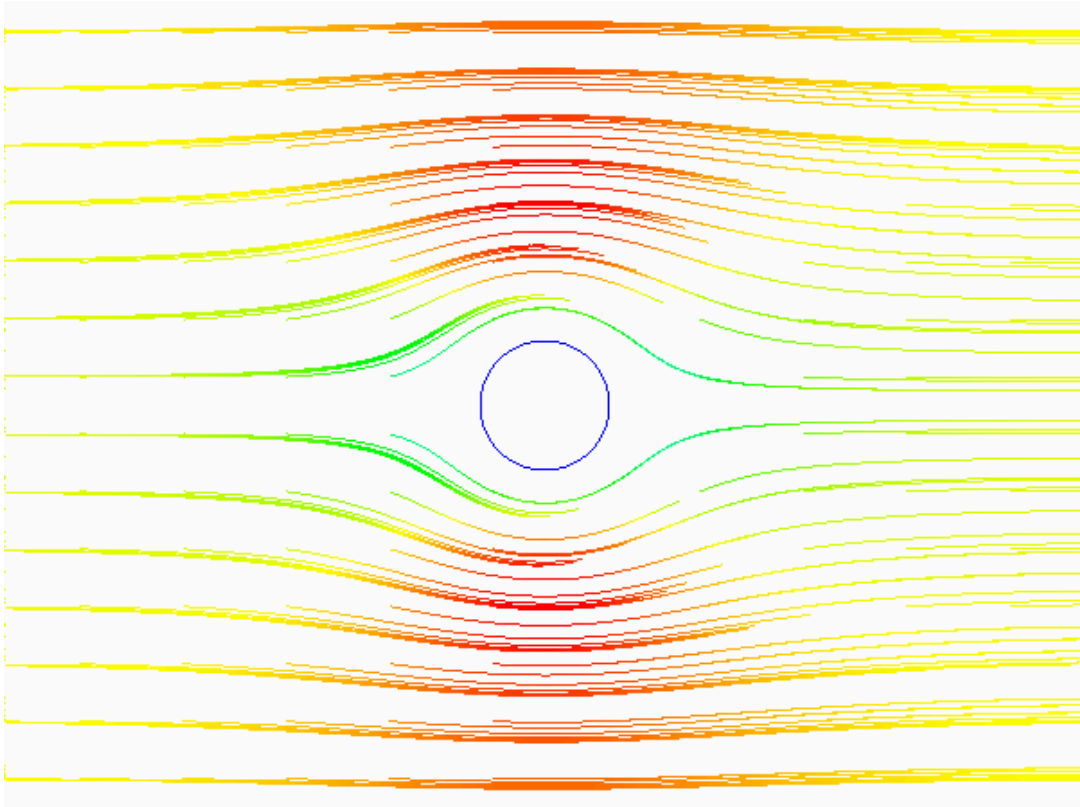


Fig.3 The velocity (the initial shape)

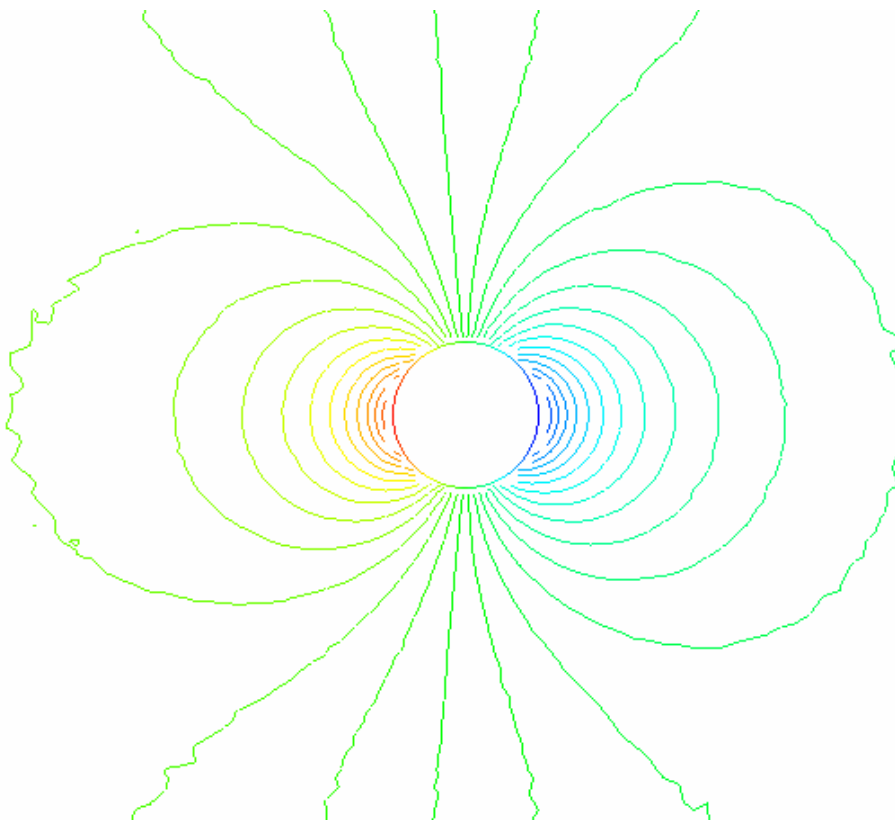


Fig.4 The pressure (the initial shape)

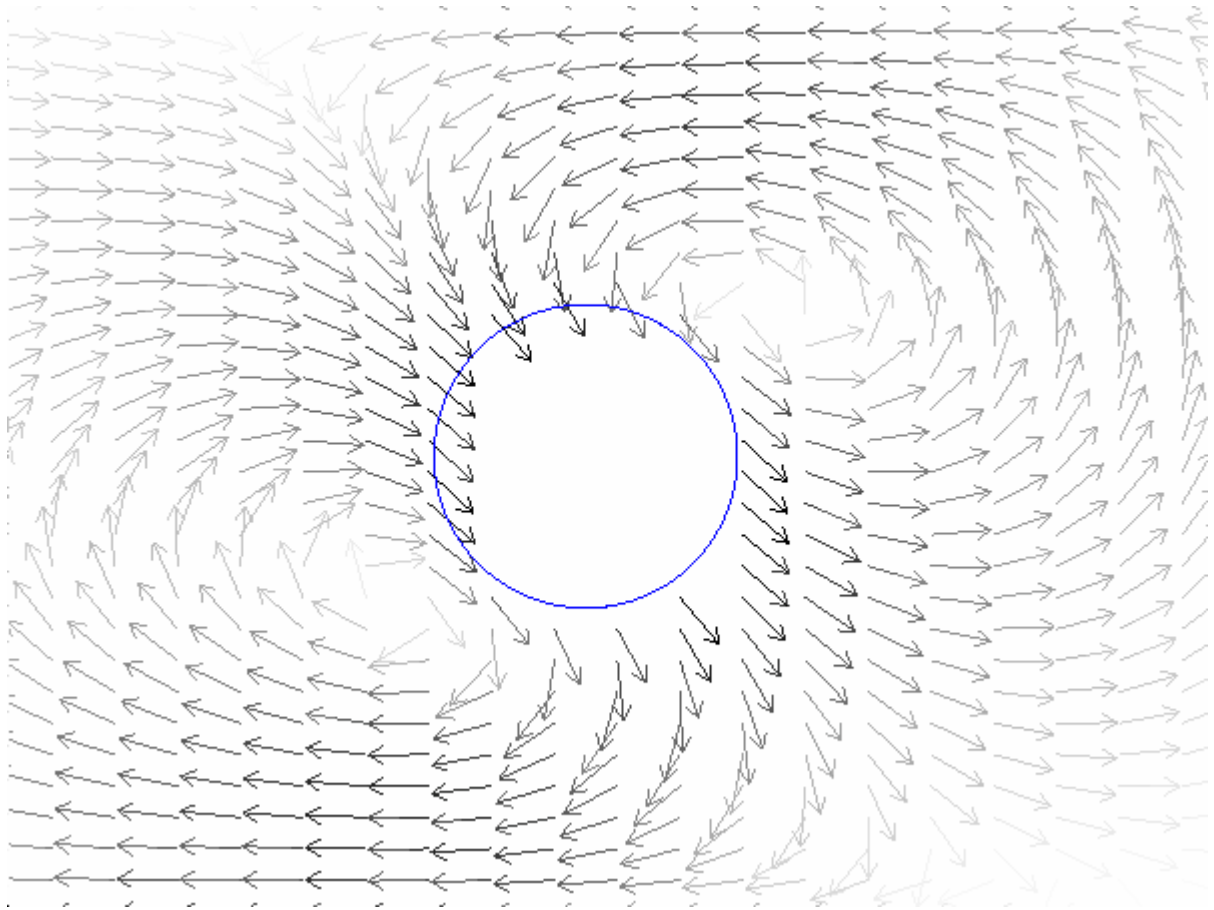


Fig.5 The adjoint velocity (the initial shape)

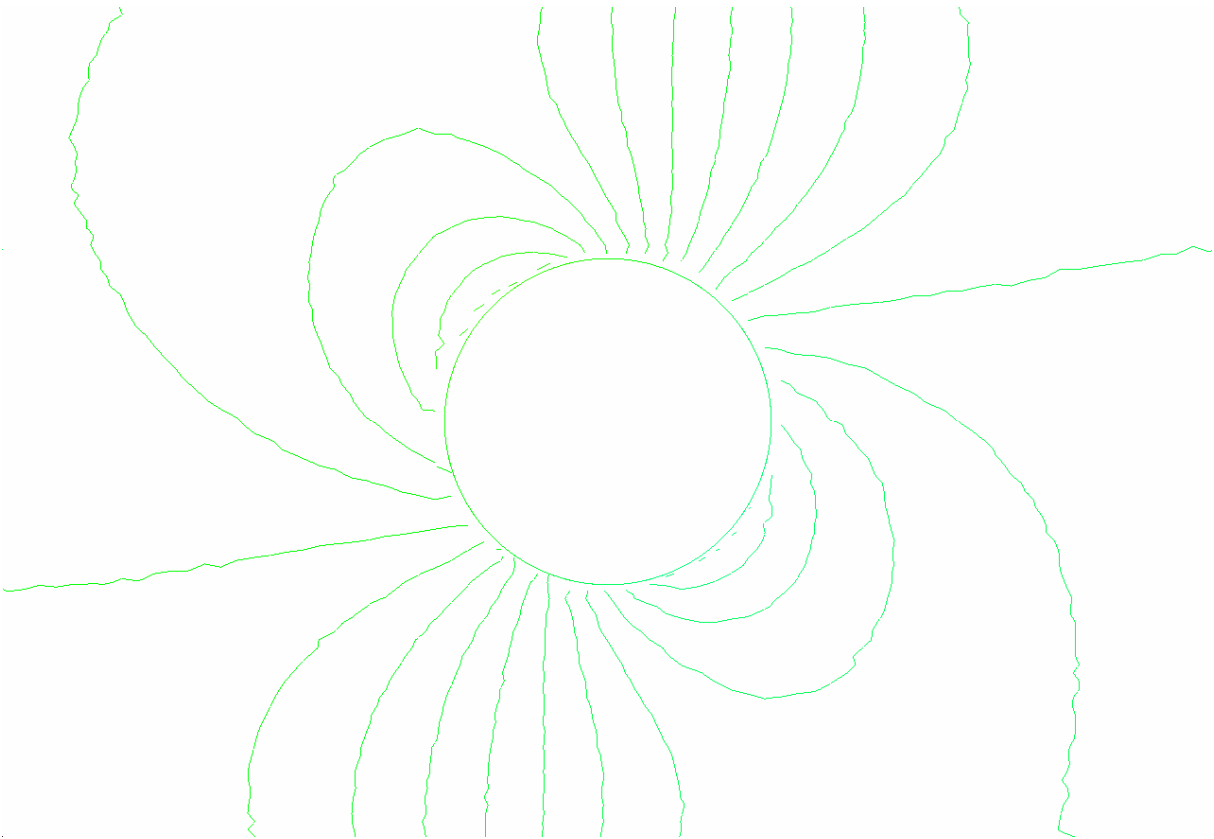


Fig.6 The adjoint pressure (the initial shape)

The sensitivity distributions and shapes with respect to the shape step are shown in Fig.7. As the shape advances from the initial shape to the optimal shape, the sensitivity becomes smaller and smaller. By making a slant with respect to the Pironneau results (Pironneau, 1973; Katamine and Azegami, 1995; Yagi and Kawahara, 2005), the initial shape converge to the optimal shape.

The adjoint velocity and pressure in the optimal shape are shown in Fig.8 and Fig.9 respectively.

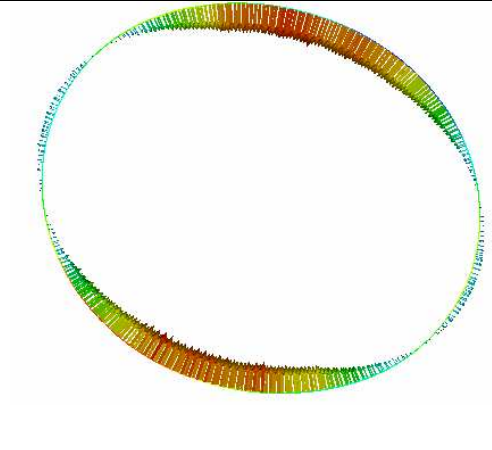
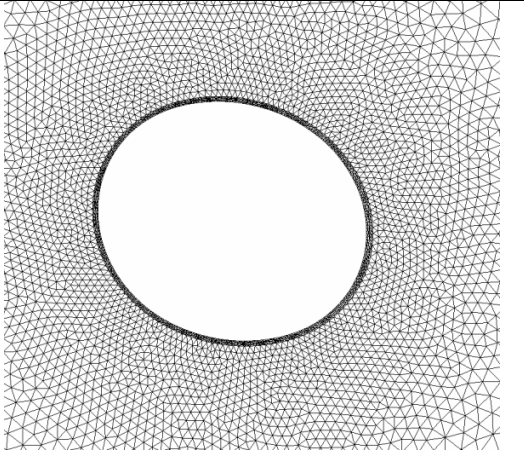
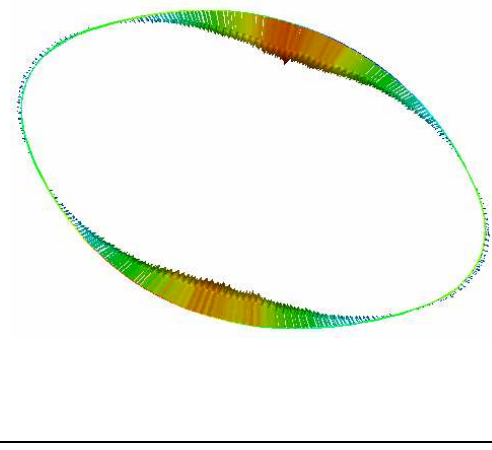
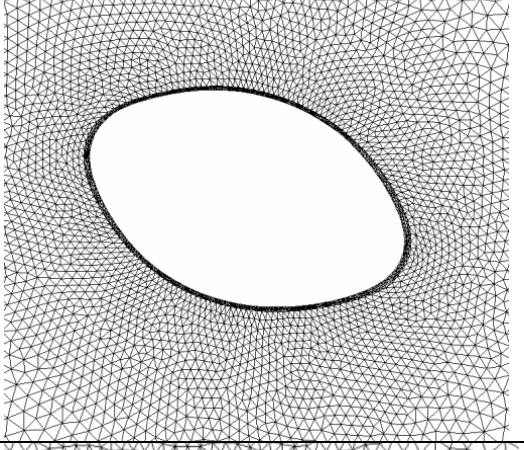
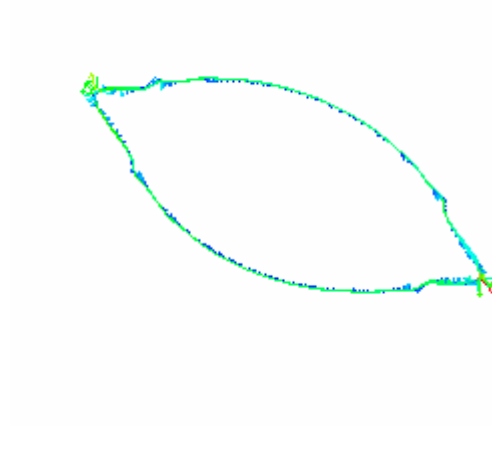
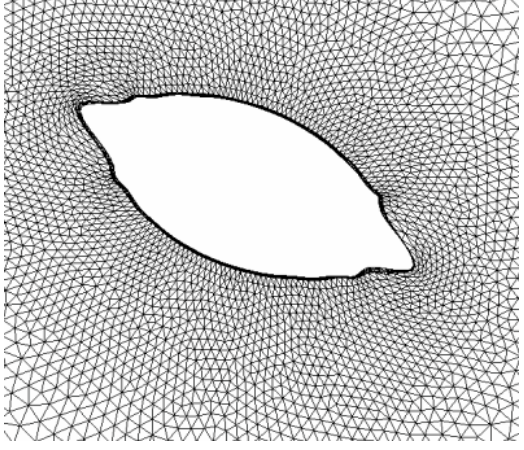
	Sensitivity distribution	Shape(view II)
Shape step 2		
Shape step 10		
Optimal Shape		

Fig. 7 The sensitivity distribution and the shape deformation with respect to shape steps

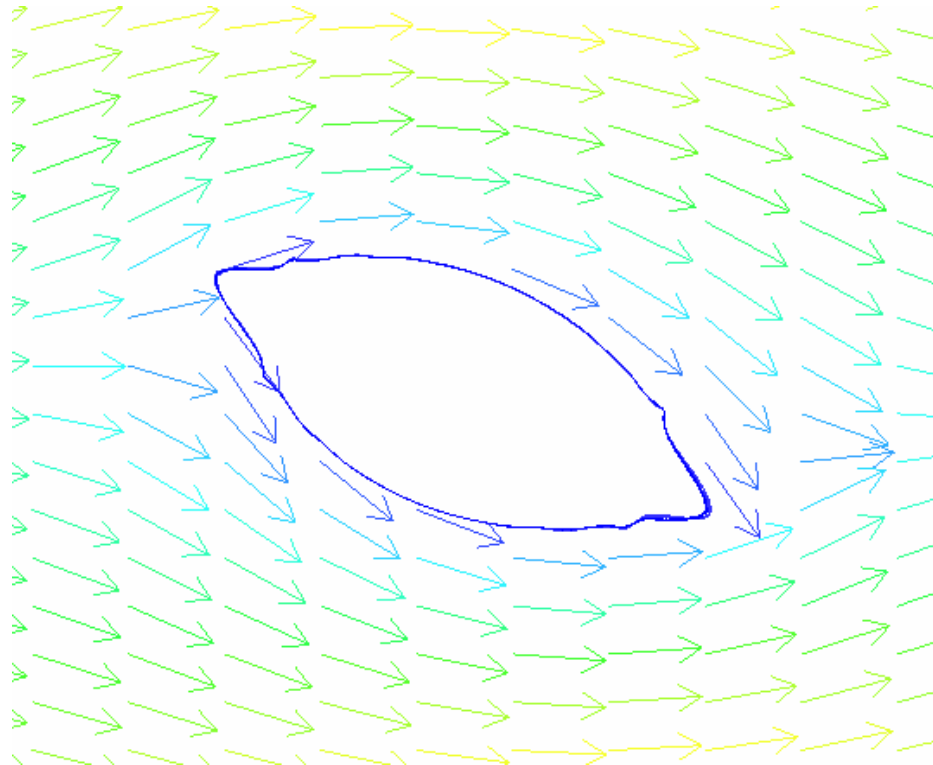


Fig.8. The velocity (the optimal shape)

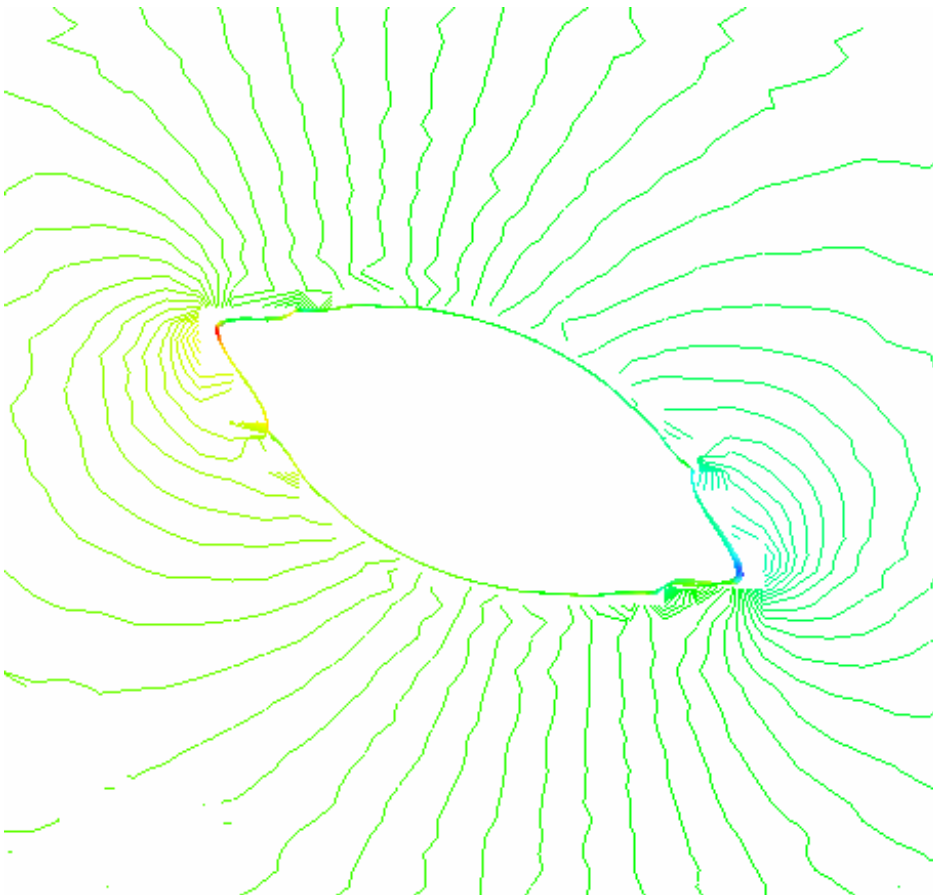


Fig.9 The pressure (the optimal shape)

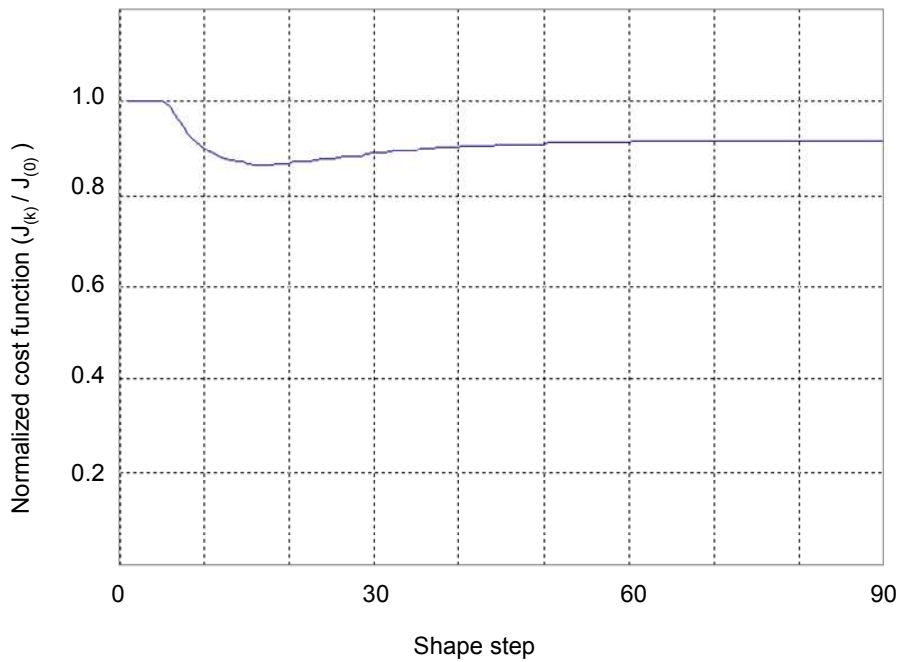


Fig 10 The history of the drag (the cost function)

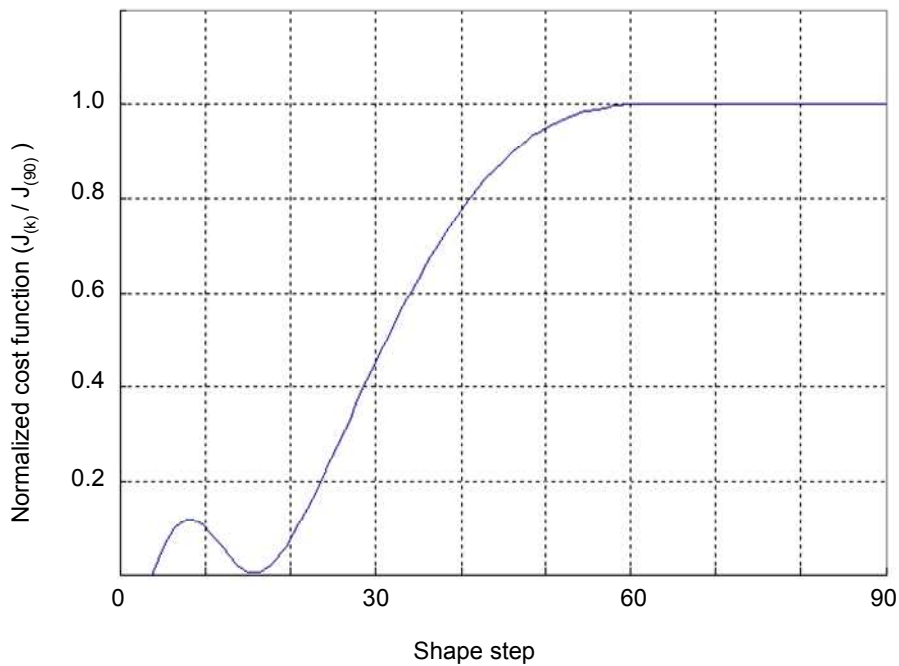


Fig 11 The history of the lift (the cost function)

The history of the drag is shown in Fig.10. The horizontal axis shows the shape step. The vertical axis shows the normalized cost function with respect to the cost function of the initial shape. The drag coefficient in the initial shape is 13.65. Comparing to the drag in the initial shape, the drag in the optimal shape is reduced by about 8%. The lift force is shown in Fig.11. The horizontal axis shows the shape step. The vertical axis shows the normalized cost function with respect to the cost function of the optimal shape. The lift coefficient increases

from the lift coefficient 0.0 in the initial shape to the lift coefficient 6.37 in the optimal shape.

5. CONCLUSIONS

To simultaneously maximize the lift and to decrease the drag of an object placed under Stokes flow, a shape optimization system based on the adjoint variable method was developed by using HEC-MW. The automatic parallel library HEC-MW used on a PC cluster made possible the computation of the optimal shape. By using the improved shape optimization system, the optimal shape under steady flow could be obtained. This method can be widely applied to both simple and complex shapes. We believe to be more efficient and robust than the conventional techniques currently used in shape optimization.

ACKNOWLEDGMENTS

This work was supported by the IML (Intelligent Modelling Laboratory). The first author is grateful to the IML for the financial support as a postdoctoral fellow. This work was also supported by the HEC-MW group (Frontier Simulation Software for Industrial Science (FSIS) project, which started in 2002 and has been driven for more than three years, has developed and released more than 60 pieces of most-advanced simulation software in the field of computational mechanics). This program, based on HEC-MW, was improved by useful advice from a large number of people, who also helped debug it. The first author gratefully acknowledges useful advice received from Serban Georgescu.

REFERENCES

- HEC-MW. <http://www.rss21.iis.u-tokyo.ac.jp/en/result/download/>.
- Hicks, R.M., Murman, E.M. and Vanderplaats, G.N. (1974), An Assessment of airfoil design by numerical optimization, *NASA Center for AeroSpace Information (CASI)*, NASA-TM-X-3092.
- Gelfand, I.M. and Fomin S.V. (1963), Calculus of variations (Translated and Edited by Richard A. Silverman), *Englewood Cliffs, N.J., Prentice-Hall*.
- Ito, S. and Okuda, H. (2007), HPC-MW: A Problem solving environment for developing parallel FEM applications. *Applied Parallel Computing. State of the Art in Scientific Computing, Lecture Notes in Computer Science, Springer Berlin / Heidelberg*, 4699; pp.694-702.
- Jameson, A. (1988), Aerodynamic design via control theory, *Journal of Scientific Computing*, 3(3), pp. 233-260.
- Katamine, E. and Azegami, H.,(1995), Domain optimization analysis of viscous flow field, *The Japan Society of Mechanical Engineers*; 61, pp.1646-1653.
- Matsumoto, J. (2004), Shape identification for Navier-Stokes equation with unsteady flow using bubble function element stabilization method, *WCCM*, 353.
- Pironneau, O. (1973), On optimum design in fluid mechanics, *Journal of Fluid Mechanics*, 59, pp.117-128.
- Robert, W. (1974), Calculus of variations. *Dover publications*.
- Shinohara, K., Okuda, H., Ito, S., Nakajima, N. and Ida, M. (2006), Shape optimization using an adjoint variable method in ITBL grid environment, *14th International Conference On Nuclear Engineering*, 89568.
- Yagi, H. and Kawahara, M. (2005), Shape optimization of a body located in low Reynolds number flow, *International Journal for Numerical Methods in Fluids*, 48, pp. 819-833.